SYSTEM CHARACTERIZATION FOR A FAST OPTICAL IMAGER

by

Uzay Emrah Emir

B.Sc., in Electrical and Electronics Engineering, Ege University, 2001

Submitted to the Institute of Biomedical Engineering
in partial fulfillment of the requirements
for the degree of
Master of Science
in
Biomedical Engineering

Boğaziçi University
2003

SYSTEM CHARACTERIZATION FOR A FAST OPTICAL IMAGER

APPROVED BY:

Yrd.Doç.Dr. Ata Akın .....
(Thesis Supervisor)

Prof. Dr. Yekta Ülgen .....

Doç. Dr. Yasemin Kahya .....

DATE OF APPROVAL: 17/06/2003

ACKNOWLEDGMENTS

First of all I would particularly like to thank my supervisor Dr. Ata Akın. He has been extremely helpful with continuous guidance and support throughout this project, and patiently proof-reading my M.Sc. thesis.

I am very grateful to Dr. Britton Chance for sharing all technical information of the CW FNIR device developed at University of Pennsylvania. I would like to express my gratitudes to Dr. Banu Onural, Dr. Kambiz Pourrezaei and Gunay Yurtsever for their collaborations and invaluable guidance.

I would also like to thank Hasan Ayaz who has developed the BRAININFO software. I am also grateful for the financial support of Boğaziçi University Research Fund, BURF 02S101.

Last, but not least, I would like to thank my family for their constant support and encouragement throughout my studies, and particularly my girl friend.

ABSTRACT

SYSTEM CHARACTERIZATION FOR A FAST OPTICAL IMAGER

In contrast to morphological imaging, functional imaging captures information about the functioning for living tissues, such as blood circulation and oxygen metabolism, cerebral nervous system, and changes in cromophore concentration. In recent years, progress in PET and MRI technologies has made these measurements possible. However both these systems are large and expensive and they have some limitations such as not being approved for use with infants in non-clinical settings and low temporal resolution. Optical imaging fills this gap by being completely non-invasive, portable, unobtrusive, low-cost, and robust to motion artifacts.

This M.Sc. thesis is involved with the development and modifications of a prototype fast optical imaging (FOI) system based on the functional near infrared spectroscopy system of University of Pennsylvania. FOI is designed by using inexpensive photodiode (PD) detectors and LEDs working in the near infrared spectrum. In addition to this a new probe design considering limitations of the preceding versions is also completed. The aim of the work was to develop a simple and robust instrument and probe to monitor brain activity, during cognitive task.

The ability and effectiveness of the system is tested by several experiments based on phantom studies. Preliminary results are promising to continue on human subjects.

Keywords: FOI, functional near infrared spectroscopy(fNIR), brain imaging, optical imaging, neuroimaging.

ÖZET

HIZLI OPTİK GÖRÜNTÜLEYİCİNİN SİSTEM ÖZELLİKLERİNİN BELİRLENMESİ

Morfolojik görüntülemeye kıyasla, işlevsel görüntüleme canlı doku işlemleri, örneğin kan dolaşımı, oksijen metabolizması, beyinsel sinir sistemi, kromofor derişimi hakkında bilgi verebilmektedir. Son yıllarda PET ve MRI teknolojilerindeki ilerleme bu işlemleri görüntülemeyi olası kılmaktadır. Tüm bunlara rağmen bu iki sistemin pahalı ve ebatça büyük olması, zamansal ayrımının düşüklüğü ve klinik dışı ortamlarda uygulanamaması bazı kısıtlamalar getirmektedir. Optik görüntüleme bu boşluğu girişimsel olmaması, ucuz, taşınabilir olma özellikleri ile doldurmaktadır.

Bu yüksek lisans tezi, Pensilvanya Üniversitesindeki emsalinden esinlenerek hızlı optik görüntüleme(HOG) sisteminin geliştirilmesini ve değiştirilmesini içermektedir. HOG sisteminin tasarımında fotodiyot algılayıcılar ve yakın kızıl ötesinde çalışan LEDler kullanılmıştır. Bu çalışmada önceki çalışmalarda görülen prob sıkıntıları dikkate alınarak yeni bir prob da geliştirilmiştir. Temel olarak bu çalışmanın amacı basit, dayanıklı bir optik görüntüleme cihazı geliştirerek, beynin işlevsel aktivitelerini gözlemlemektir.

Geliştirilen cihazın teknik özellikleri çeşitli fantom deneyleri ile test edilmiştir. İlk bulgular insan üzerinde de ölçüm alınabileceğini gösteren sonuçlar içermektedir.

Anahtar Sözcükler: HOG, İşlevsel yakın kızıl ötesi spektroskopi, Beyin görüntüleme, Optik görüntüleme, Sinir görüntüleme.

TABLE OF CONTENTS

LIST OF FIGURES

LIST OF TABLES

LIST OF SYMBOLS

I_0	Incident light intensity
I_L	Transmitted light intensity
OD	Optical Density
λ	Wavelength
$\varepsilon(\lambda)$	Absorption coefficient as a function wavelength
C	Concentration
L	Mean free pathlength
$B(\lambda)$	Correction of mean free pathlength with respect to wavelength
n_{det}	Photodetector(Photodiode) noise when the LEDs are off
n_{env}^{on}	Added noise when the LEDs are on
n_{env}^{off}	Sum of the background noise
N_d	Noise intensity
μ_a	Absorption Coefficient
μ_s	Scattering Coefficient
$\lambda\#$	Wavelength Number
$Q\#$	Quadrant Number
$PD\#$	Photodiode Number

LIST OF ABBREVIATIONS

FOI	Fast Optical Imaging
PET	Positron Emission Tomography
fMRI	Functional Magnetic Resonance Imaging
BOLD	Blood Oxygenation Level-dependent
fNIR	Functional Near Infrared Spectroscopy
MEG	Magnetoencphalography
SPET	Single-positron Emission Tomography
EEG	Electroencephalography
CBF	Cerebral Blood Flow
CBV	Cerebral Blood Volume
Hb	Deoxy-hemoglobin
HbO_2	Oxy-hemoglobin
NIR	Near Infrared
TPSF	Temporal point Spread Function
TCSPC	Time-correlated Single Photon Counting
PMT	Photomultiplier Tube
APD	Avalanche Photodiode Detector
OTDR	Optical Time Domain Reflectometer
CW	Continuous Wave
FD	Frequency Domain
TR	Time Resolved
PDF	Probability Density Function
DOT	Diffuse Optical Tomography
MRI	Magnetic Resonance Imaging

1. INTRODUCTION

1.1 Motivation and Objectives

Understanding functional organization of the normal human brain, by using techniques to assess changes in brain circulation has occupied scientists for more than a century. At this point, cognitive neuroscience has emerged as a very important growth area in neuroscience. Cognitive neuroscience gathers the experimental strategies of cognitive psychology with various techniques to actually examine how brain function supports mental activities [1]. Among the new techniques of functional brain imaging used in these experiments in normal humans are positron emission tomography (PET), functional magnetic resonance imaging (fMRI), and recently fast optical imaging (FOI).

Fast Optical Imaging is in many ways an extension of functional near infrared spectroscopy, which is now routinely used in laboratory and clinical studies. Primarily, it aims to measure global changes in tissue oxygenation and blood volume. It provides a useful tool to complement existing medical imaging modalities by exploiting the harmless non-ionizing radiation. Patients can be examined repeatedly, or even continuously with FOI system. Optical systems measure changes in cerebral blood volume or oxygenation without causing any irreversible structural damage. FOI is shown to have several advantages in terms of temporal resolution, low cost and portability compared with conventional techniques.

The objective of my M.Sc. project is to make a major contribution to the development of a modified duplicate of a continuous wave fast optical imaging system at Boğaziçi University to enable brain neuroimaging studies. The work involves completing its construction, evaluating the instrument performance, and performing preliminary phantom studies.

1.2 Outline of the Thesis

In writing this thesis I have attempted to provide a thorough background of the medical, physical and technological aspects of available optical brain imaging systems. A large section of the thesis is dedicated to discussion of the system's design features and performance characteristics. Finally, the experimental procedures and results from initial phantom measurement are described. However human brain activation measurements have not been performed yet.

Chapter 2 contains a description of the physiology of the human brain in general and provides descriptions of the established medical imaging systems and clinical needs.

Chapter 3 provides a general introduction to the physics and mathematics of light propagation through biological tissue and summarizes the history and current state of NIR spectroscopy and imaging systems. The most common types of instruments are reviewed, and compared.

Chapter 4 begins with a discussion of the system design considerations and requirements. A brief explanation of the functioning of the instrument as a whole is followed by a detailed description of the individual optical and electronic assemblies, as well as the control software. It also focuses on performance of the individual components and their experimental setup.

Finally, Chapter 5 provides a discussion of the work done so far and the prospects for the future of this project and medical optical imaging in general.

2. FUNCTIONAL NEUROIMAGING

2.1 Clinical Need For Functional Neuroimaging

An essential characteristic of neurological disorders, mental illness, and drug abuse is a dysfunction of cognitive processes. In order to understand these disorders, systematic experiments and observations are important. The methodical study of normal cognitive processes in humans and animals is necessary in understanding these disorders. With the development of invasive and non-invasive functional neuroimaging techniques, new opportunities have been offered for studying the neural control, representation and expression of cognitive functions in the alert, normal human . Both positron emission tomography (PET) and functional magnetic resonance imaging (fMRI) techniques have been used extensively to investigate cognitive function. Within the last decade, optical neuroimaging has been used for noninvasive imaging of human brain function as well. With the help of these techniques, new opportunities have been provided to ask questions concerning the neural correlates of cognitive function, limitations in their temporal and spatial resolution have led to constraints on the specific nature and the design of the experimental questions that can be asked.

Many studies have been performed in localizing the role of various brain areas in attention, perception, language processing and generation, learning and memory mechanisms, and emotions. The type of technique is chosen according to the specific physiologic measurement e.g., blood oxygenation/deoxygenation for the blood oxygenation level-dependent (BOLD) fMRI technique, cerebral blood flow for PET technique or the change in absorption of photons of particular wavelengths in intrinsic optical signals. An important issue in the interpretation of these studies has been the relationship between these measurements and the neural activity hypothesized to underlie these changes. As neuroscience research increasingly focuses on the specific brain loci relevant to the pathology of various diseases and the underlying basis of various cognitive functions, it is increasingly important to determine the actual functional relationship

between the images generated by these tools and the underlying neural activity in the relevant areas of the central nervous system [2].

2.2 Techniques of Neuroimaging

There are several non or minimally invasive neuroimaging methods that are readily available to clinical neuroscientists for neuroimaging. Historically, first electroencephalography (EEG) appears, it is followed by other technologies such as positron emission tomography (PET)/single-positron emission tomography(SPET), magnetoencephalography (MEG), functional magnetic resonance imaging and most recently functional optical imaging. These methods are often classified in terms of whether they provide direct or indirect information about brain function.

Direct methods include MEG, EEG, and event-triggered EEG (also called event related potentials; ERPs), each of which monitors a direct consequence of brain electromagnetic activity.

In particular, EEG measures brain function by analyzing the scalp electrical activity generated by brain structures. It is a completely noninvasive procedure that can be applied repeatedly in patients, normal adults, and children with virtually no risks or limitations. Local current flows are produced when brain cells (neurons) are activated. However, only electrical activity generated by large populations of neurons concurrently active can be recorded on the head surface [3].

As for MEG, the electric current in a group of neurons that is situated closely together can be viewed as a single source of current. The magnetic field over the surface of the head may be measured by an array of detectors and used to determine the precise position and strength of the source within the brain (Figure 2.1) [4].

On the other hand, indirect method includes PET/SPET, fMRI that usually

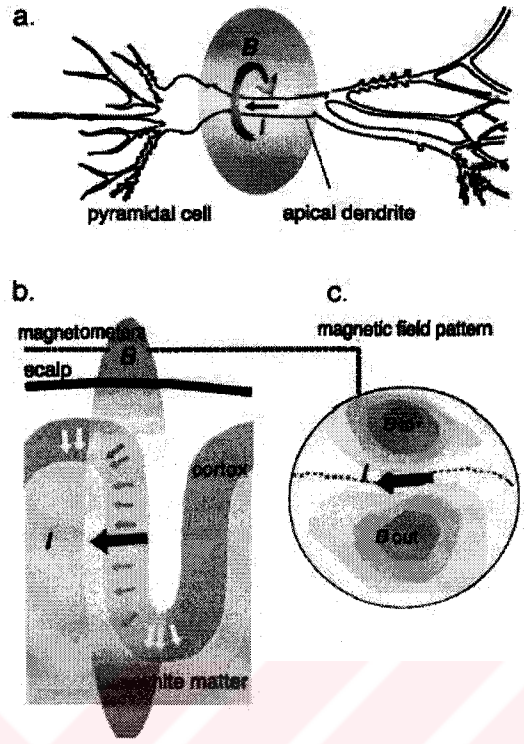

Figure 2.1 MEG principle [4].

monitor hemodynamic changes consequent to brain electrical activity.

PET depends on detecting positrons emitted radio labeled tracers injected into the blood stream. Using different isotopes, the physiological parameters of cerebral blood flow (CBF) and cerebral blood volume (CBV) can be determined. PET has the advantage that the biological variables can be calibrated in terms of absolute physical quantities such as metabolic rates in mg of a substance consumed per minute per unit volume of tissue. The main disadvantages come from the reliance on radioactivity (Figure 2.2(a)) [2].

MRI is based on the nuclear magnetic resonance of hydrogen atoms (protons) in water. When protons are placed in a strong magnetic field and exposed to a pulse of radio waves of a particular frequency, they resonate or emit energy of the same frequency. The resonance signal can be spatially localized by applying magnetic-field gradients in three dimensions and the localized signals can be converted to an anatomical image. Because the signal contains information about whether the hydrogen atoms

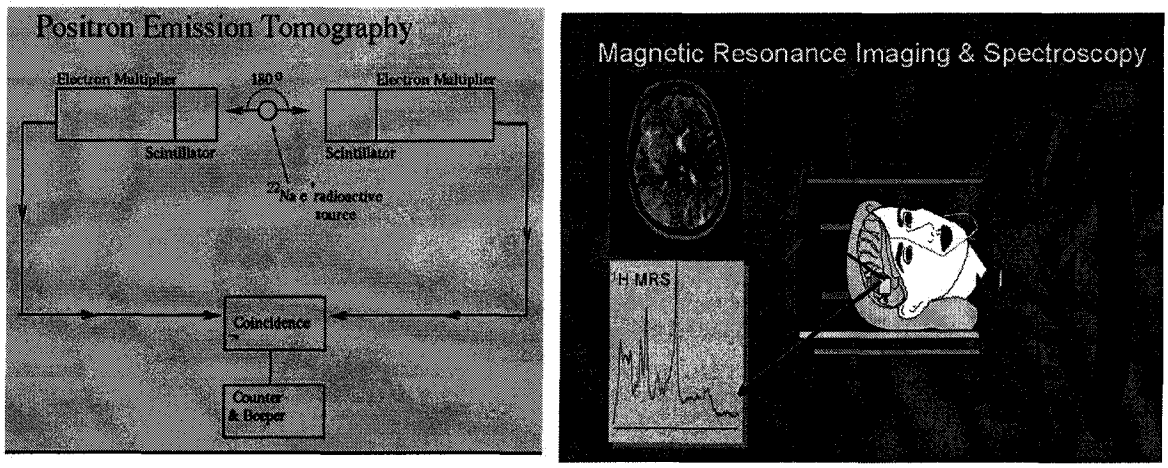

(a) (b)

Figure 2.2 (a)PET principle.(b)fMRI principle [2]

are present as free water or are partially bound in molecular structures such as fat, muscle or blood, MRI can differentiate various tissue types. Thus it reveals excellent anatomical detail, particularly of soft tissues. fMRI, in contrast, monitors changes in local brain activity by measuring signals that depend on the differential magnetic properties of oxygenated and deoxygenated hemoglobin, termed the blood oxygen level dependent (BOLD) signal, which gives a measure of changes in O_2 availability (Figure 2.2(b)) [2].

2.3 Physiological Events During Brain Activation

Plenty of clinical evidence indicates that brain is exquisitely sensitive to perturbations in energy metabolism. Careful consideration of the basic mechanisms of neuron activation metabolism is essential to a full understanding of the physiology of brain function.

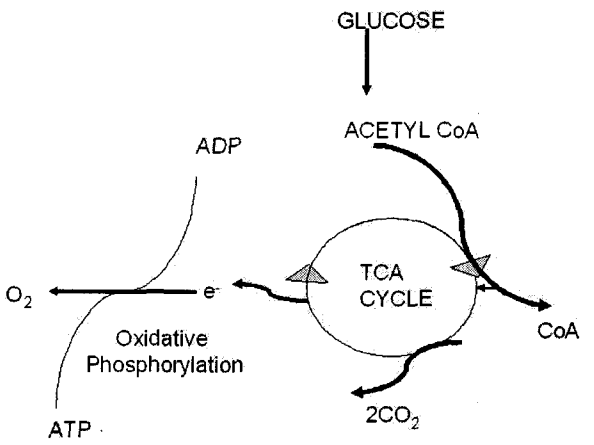

Figure 2.3 Overview of the aerobic metabolism of glucose to ATP following the Kreb's cycle [5].

2.3.1 Metabolism and Blood Flow in the Brain

The brain, like any other organ in the body requires a steady supply of oxygen in order to metabolize glucose to provide energy. This oxygen is supplied by the component of the blood called hemoglobin. The biochemical reactions that transmit neural information via action potentials and neurotransmitters require energy. Glucose, in normal circumstances, is the main energy substrate of the brain [6]. This energy is provided in the form of ATP, which in turn is produced from glucose by oxidative phosphorylation and the Kreb's cycle (Figure 2.3).

As ATP is hydrolyzed to ADP, energy is given up, which can be used to drive biochemical reactions that require free energy. The production of ATP from ADP by oxidative phosphorylation is governed by demand, so that the energy reserves are kept constant. That is to say, the rate of this reaction depends mainly on the level of ADP present. This means that the rate of oxygen consumption by oxidative phosphorylation is a good measure of the rate of use of energy in that area (Figure2.4(a),2.4(b)) [5]. This oxygen is supplied in the blood. Since oxygen is not very soluble in water, the blood contains a protein that oxygen can bind to, called hemoglobin. When an oxygen molecule binds to hemoglobin, it is said to be oxyhemoglobin, and when no oxygen is bound it is called deoxyhemoglobin. The demand for glucose and oxygen by neuronal tissues is responded by the increase in cerebral blood flow to a localized region of

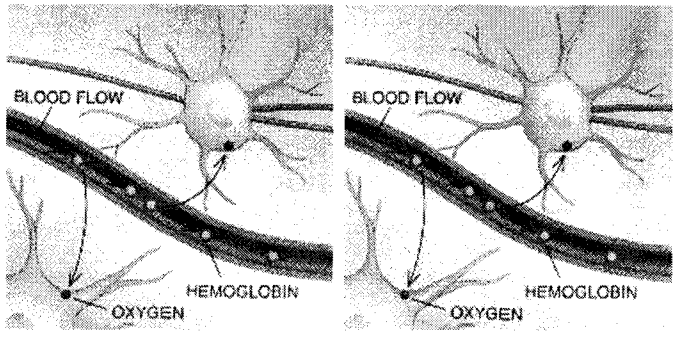

(a) (b)

Figure 2.4 Upon activation, oxygen is extracted by the cells, thereby increasing the level of deoxyhemoglobin in the blood. This is compensated for by an increase in blood flow in the vicinity of the active cells, leading to a net increase in oxyhemoglobin [5].

brain tissue. The increase in blood flow can be monitored indirectly by measuring the changes in oxy and deoxyhemoglobin concentrations via FOI(fNIR)method.

2.4 Functional Optical Imaging

Optical neuroimaging is a rapidly developing method which has provided enormous information about the mechanisms of damage in the neonatal brain, and the functional development and process of both the normal and abnormal brain.

Optical imaging of the human brain is possible because there is a *window* of transparency of biological tissue to light in the near infrared part of the spectrum. Near-infrared (NIR) light from approximately 650-950 nm is even more weakly absorbed by tissue than the red wavelengths. In Figure 2.5(a), light in the optical window is able to penetrate tissues, so that it can be used to measure hemoglobin concentration in the brain, and deduce cerebral blood volume [7]. In addition, oxyhemoglobin (HbO_2) and deoxy-hemoglobin (Hb) have different absorption characteristics, so that changes in blood oxygenation can be measured. All of the optical neuroimaging techniques are based on the same model -shine light onto the scalp, detect it as it exits the

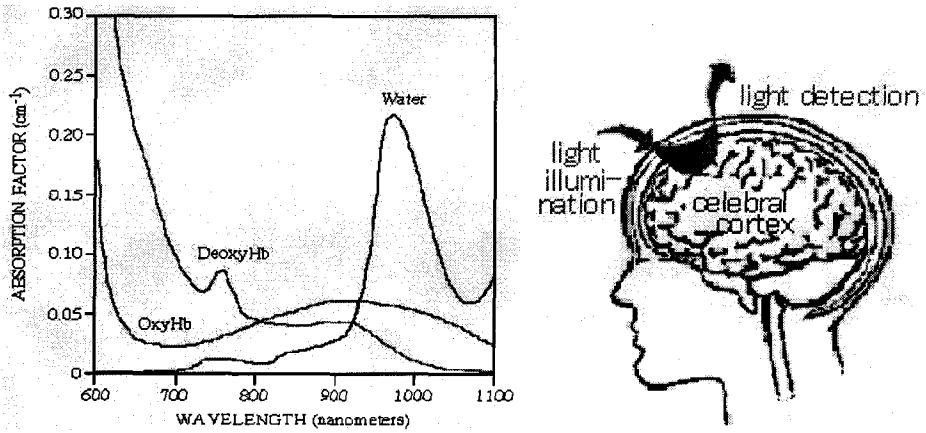

(a) (b)

Figure 2.5 (a)The Absorption spectrum of cromophores (b)Model of optical neuroimaging[8]

head, and use the absorption spectra of the light absorbing molecules (chromophores) present in tissue to interpret the detected light levels as changes in chromophore concentrations(Figure 2.5(b)).

Table 2.1 summarizes the spatial and temporal sensitivity of these various neuroimaging techniques.

Table 2.1
Comparison of neuroimaging techniques[9].

Technique	Spatial Resolution	Temporal Resolution	Physiological Measurements
SPECT	10 mm	Tens of seconds	cerebral blood flow
PET	5 mm	Tens of seconds	cerebral blood flow
EEG	poor	1 ms	electrical activity
MEG	5 mm	1 ms	magnetic activity
fMRI	3 mm	50 to 100 ms	deoxygenated hemoglobin(Hb)
FOI	20 mm	Milliseconds to tens of seconds	Hb and HbO_2

In the neuroimaging arena, diffuse optical techniques are not as common as other methods. However they have been applied in several of fields of clinical neuroscience and neuroimaging. One of the first clinical applications of optical neuroimaging for

functional neuromonitoring was the investigation of fetal, neonatal and infant cerebral oxygenation and functional activation[10].

FOI, also called functional near infrared spectroscopy (fNIRS), has been most successfully applied to the study of extremely premature infants. CBF is low in preterm infants, and increases over the first 3 days of life as part of the normal adaptive response to extrauterine life. Low CBF during this period is associated with an increased risk of both intraventricular hemorrhage and periventricular leukomalacia, with subsequent neurodevelopmental impairment. FOI has been adapted to enable outside measurement of cerebral oxygen saturation. FOI is also used in assessment of perinatal asphyxia. When the newborn brain is subjected to a hypoxic-ischemic insult, its circulation becomes vasodilated. This can be very clearly measured using FOI whereby measurements of cerebral blood volume are correlated with both the degree of encephalopathy and the severity of neurodevelopmental impairment [10].

3. FUNCTIONAL OPTICAL IMAGING SYSTEM

Optical imaging techniques are rapidly developing in medicine. As it was pointed out earlier, the potential advantage of optical over other conventional medical imaging techniques is the unique combination of non-ionising radiation, the potential to differentiate between different types of soft tissue, and the possibility to derive functional information from quantitative measurements of chromophore concentrations. This section provides information about tissue optics, various methods used in optical imaging systems, developed systems and need for modifications that have been made in this thesis.

3.1 Tissue Optics

Biological tissues are optically inhomogeneous and absorbing media whose average refractive index is higher than that of air. This is responsible for partial reflection of the radiation at the tissue/air interface, while the remaining part penetrates the tissue. Multiple scattering and absorption are responsible for light beam broadening and eventually decay as it travels through tissue, but bulk scattering is a major cause of the dispersion of a large fraction of radiation in the backward direction. Cellular organelles such as mitochondria are the main scatterers in various tissues [11].

3.1.1 Absorption

Absorbed light is converted to heat or radiated in the form of fluorescence. It is also consumed in photobiochemical reactions. Absorption is wavelength dependent and its spectrum depends on the type of predominant absorption centers and water content of tissues. The absorption of light intensity in a non-scattering medium is described by the Beer-Lambert Law (Eq. 3.1). This law states that for an absorbing compound

dissolved in a non-absorbing medium:

$$I_L = I_0 e^{-\varepsilon(\lambda)CL} \tag{3.1}$$

where I_0 is the incident light intensity, I_L is the transmitted light intensity through the medium, $\varepsilon(\lambda)$ is the absorption coefficient as a function of wavelength, C the concentration of the absorber, and L is the optical pathlength (distance from source to detector). This equation can be arranged to yield direct information on C, the concentration of the absorber, as:

$$OD(\lambda) = \log(I_0/I_L) = \varepsilon(\lambda)CL \tag{3.2}$$

where OD is the optical density.

A compound which absorbs light in the spectral region of interest is known as a chromophore. Each chromophore has its own particular absorption spectrum which describes the level of absorption at each wavelength. The principle chromophores in tissue are outlined below:

3.1.1.1 Water. As shown in figure 3.1, the absorption of light by water is relatively low between 700 - 900 nm. Beyond 900 nm absorption starts to rise with increasing wavelength and peak value is at 970 nm. The high concentration of water in living tissue, typically 80% in adult brain tissue determines the wavelength region in which spectroscopic examination of tissue is possible by strongly limiting the tissue thickness through which light can penetrate. For this reason, the water spectrum is said to demonstrate a " window " of transparency between 200 and 900 nm within which spectroscopic measurements can be made for the purposes of most clinical measurements of the water concentration in tissue [11, 12].

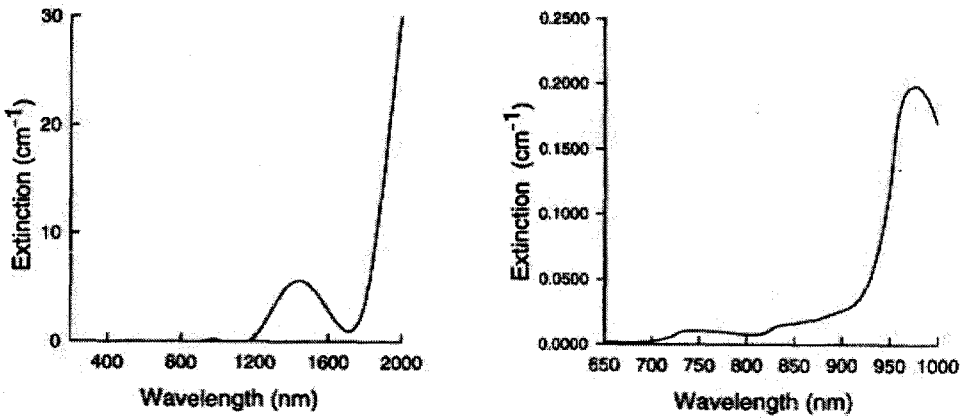

Figure 3.1 The absorption spectra of pure water [12].

3.1.1.2 Lipid. Although the distribution of lipid in tissue is dependent upon tissue type, it can also be thought of as a constant absorber with changes in its concentration throughout the course of a clinical measurement being unlikely. The absorption spectrum of lipid is approximately the same as that of water and it can involve 10-40% of tissue [11, 12].

3.1.1.3 Melanin. Melanin, found in the epidermis layer of skin, is a highly effective absorber of light, especially in the ultraviolet region of the spectrum. Although this absorption can be considered to be constant and oxygen independent, the concentration of melanin in tissue will directly affect the reflectance of light from the skin and therefore the transmission of light into the tissue below [11, 12].

3.1.1.4 Hemoglobin. Figure 3.2 shows the specific extinction coefficients of oxygenated hemoglobin (HbO_2) and deoxyhemoglobin (Hb) in the wavelength range 450 - 1000 nm. The difference in the absorption spectra explains the well recognized phenomena of arterial blood (containing approximately 98% HbO_2) having a bright red appearance while venous or deoxygenated blood appears more blue. In the NIR region of the spectrum the absorption of both chromophores decreases significantly compared to that observed in the visible region. However the absorption spectra of Hb and HbO_2 remain significantly different in this region allowing spectroscopic separation of

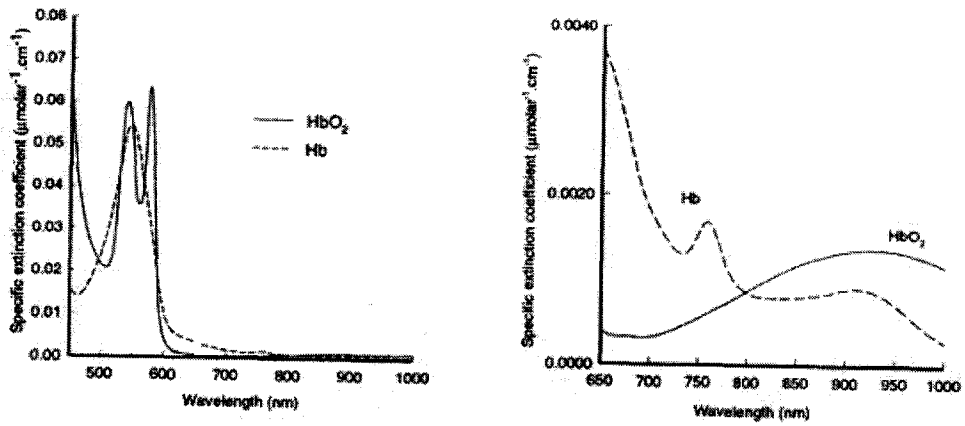

Figure 3.2 The absorption spectra of HB and HBO [12].

the compounds to be possible using only a few sample wavelengths. An isobestic point where the specific extinction coefficients of the two compounds are equal can be seen at around 800 nm, which can be used to calculate hemoglobin concentration independent of oxygen saturation [11, 12].

3.1.2 Modified Lambert Beer Law, Hb, HbO_2 calculations

Beer Lambert law is widely used in chemical spectroscopy, and defines attenuation of light in units of optical density (Eq. 3.2). Attenuation (OD) is measured by comparing the incident light intensity (I_o) against the intensity of the emerging transmitted light (I_L) and expressing this as the number of orders of magnitude that the light intensity has been reduced when traversing the medium.

In order to determine the contribution of multiple chromophores (e.g., oxy and deoxyhemoglobin), we must take measurements at one or more wavelengths per chromophore to be resolved. For example, by measuring the change in light intensity at two wavelengths, and using the known extinction coefficients of HbO_2 and Hb at those wavelengths (in Figure 2.5(a)), one can then separately determine the concentration changes of $Hb0_2$ and Hb by solving the two equations with two unknowns for $[Hb]$ and

$[HbO_2]$ (Eq. 3.3, 3.4). This approach can be generalized to more than two wavelengths.

$$\Delta OD(\lambda_1) = (\varepsilon_{\mathrm{HbO_2}}(\lambda_1)\Delta[\mathrm{HbO_2}] + \varepsilon_{\mathrm{Hb}}(\lambda_1)\Delta[\mathrm{Hb}])LB(\lambda_1) \tag{3.3}$$

$$\Delta OD(\lambda_2) = (\varepsilon_{\mathrm{HbO_2}}(\lambda_2)\Delta[\mathrm{HbO_2}] + \varepsilon_{\mathrm{Hb}}(\lambda_2)\Delta[\mathrm{Hb}])LB(\lambda_2) \tag{3.4}$$

These equations represent the changes in the total light attenuation signal with respect to extinction coefficients (absorption coefficients) of the corresponding tissues. L is the mean free pathlength and $B(\lambda)$ is the correction of this pathlength with respect to wavelength. Given equations 3.3 and 3.4, and assuming $B(\lambda_1) \cong B(\lambda_2) = B$, $\Delta[\mathrm{HbO_2}]$ and $\Delta[\mathrm{Hb}]$, the changes in $[\mathrm{HBO_2}]$ and [Hb] concentrations; respectively, can be calculated from equations 3.3 and 3.4 as:

$$\Delta[Hb] = \frac{OD(\lambda_1) - \frac{\varepsilon_{HbO_2}(\lambda_1)}{\varepsilon_{HbO_2}(\lambda_2)}OD(\lambda_2)}{LB[\varepsilon_{Hb}(\lambda_1) - \varepsilon_{Hb}(\lambda_2)\frac{\varepsilon_{HbO_2}(\lambda_1)}{\varepsilon_{HbO_2}(\lambda_2)}]} \tag{3.5}$$

$$\Delta[HbO_2] = \frac{OD(\lambda_1) - \frac{\varepsilon_{Hb}(\lambda_1)}{\varepsilon_{Hb}(\lambda_2)}OD(\lambda_2)}{LB[\varepsilon_{HbO_2}(\lambda_1) - \varepsilon_{HbO_2}(\lambda_2)\frac{\varepsilon_{Hb}(\lambda_1)}{\varepsilon_{Hb}(\lambda_2)}]} \tag{3.6}$$

from which total blood volume change and oxygenation can be estimated by:

$$\Delta[BV] = \Delta[HbO_2] + \Delta[Hb] \tag{3.7}$$

$$\Delta[Oxy] = \Delta[HbO_2] - \Delta[Hb] \tag{3.8}$$

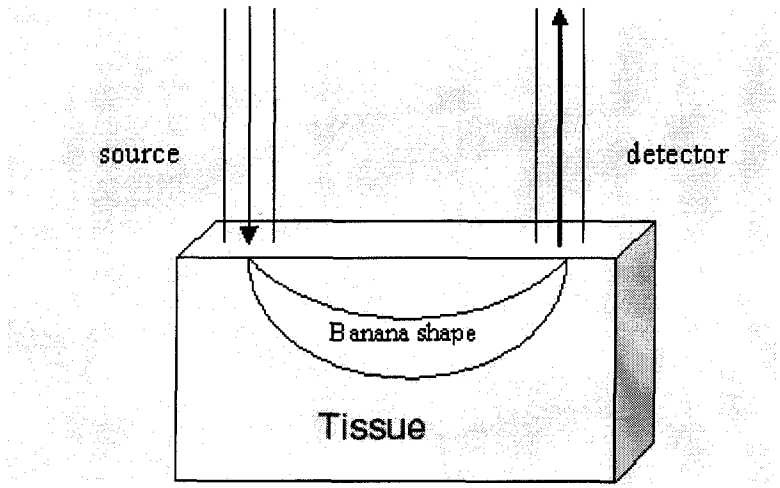

Figure 3.3 An illustration of light pathway in tissue [11].

3.1.3 Scattering

Scatter of light in tissue is due to the spontaneous variations in the refractive index at microscopic and macroscopic scales. This occurs at membrane boundaries of the cells themselves as well as at boundaries between various organelles inside the cell. As with absorption, the volume of a particular scatterer within the tissue is as important as its scattering ability [11]. Facts suggests that cell membranes are the most important source of scattering in brain tissue since they account for a large proportion of the solid content of the tissue. The effect of scattering is to increase the pathlength traveled by photons within tissue, and so as to significantly increase the probability of absorption. For many tissues, in vivo measurements are possible only in the geometry of the backscattering and we have to know from what depth the optical signal is coming. Depth is defined by the photon path distribution function for the photon migration from a source to a detector. The spatial distribution function for homogeneous scattering medium has been simulated as a banana shape (Figure 3.3) [11].

3.2 Current Functional Optical Imaging Systems

Several types of FOI systems are now commercially available. Three main methods of fNIRS have been developed: continuous wave (CW), frequency domain (FD) and time resolved (TR) (Figure 3.4).

3.2.1 Continuous Wave

The continuous wave (CW) method measures only the intensity of light. It is very reliable, but currently allows only relative or trend measurements due to the lack of information available about path length. To indicate this problem in current CW instruments, multiple separations of probes placed around the head operating simultaneously are required. This allows for a pathlength correction, but only for a homogeneous brain. The signal to noise ratio is reasonable with this technique. The depth of brain tissue which can be measured from the surface is varied typically from 1-3 cm [9, 12, 13].

3.2.2 Frequency Domain

The frequency domain (FD) method has recently been proposed for optical measurement in scattering media. The method is designed to evaluate the dynamic response of scattered light intensity to modulation of the incident light beam intensity in a wide frequency range, usually in tissue research using 50 to 1000 MHz. The FD method measures the phase and amplitude shifts. Compared with other techniques, this method is more reliable in terms of data interpretation and immunity from noise. These happen because FD equipment involves amplitude modulation at low peak powers, slow rise time and hence smaller bandwidths then the time domain methods. However, the FD technique suffers from the simultaneous transmission and reception of signals and requires attempts to avoid unwanted crosstalk between the transmitted and detected

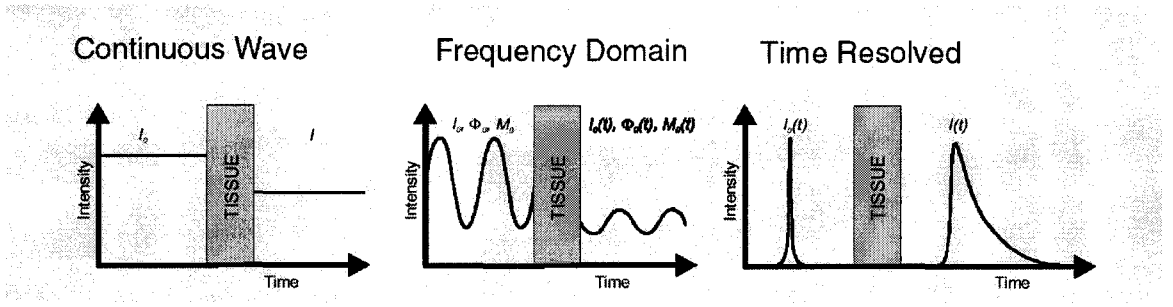

Figure 3.4 Optical Imaging Methods [12].

signals [9, 12, 13].

3.2.3 Time Resolved

The main principle of enhanced viewing through a tissue using a time resolved (TR) method is illustrated in figure 3.4. Time-resolved and intensity modulated data are Fourier transform equivalent. Time-resolved instruments measure the temporal response of tissue to an ultrashort (a few ps) input laser pulse. The temporal distribution of light emerging from the tissue surface is commonly detected with either a synchroscan streak camera, or a time-correlated single photon counting (TCSPC) system. In the latter case a photon counting detector records individual photons and measures their flight times relative to a reference pulse. Thus a histogram of the distribution of arrival times (also called temporal point spread function or TPSF) is built up. TPSFs can be interpreted as the impulse response of the tissue probed for a given source/detector probe arrangement, their shape and temporal offset depending on the optical properties within the medium. It has been shown that if the complete TPSF is recorded at a fixed probe spacing, values for μ_a and μ_s can be obtained from fits to a light transport model. Measurements at multiple wavelengths allow estimates of tissue chromophore concentrations to be made [9, 12, 13].

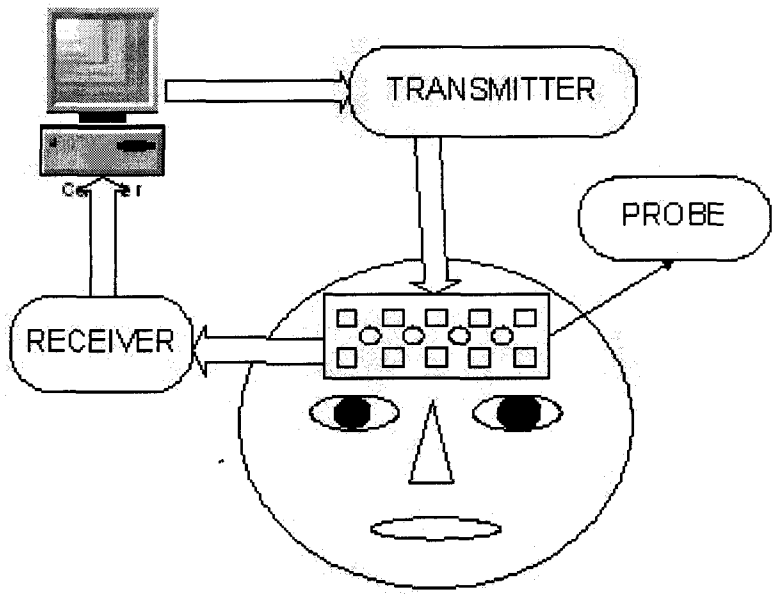

Figure 3.5 A picture of CW FOI

3.3 State of Art in FOI Systems

This section compares the optical imaging methods mentioned before and introduces the medical optical imaging systems that are currently in use by other research groups.

A FOI system (functional near infrared spectroscopy system) typically has 4 units: 1) Probe that houses the optodes (LEDs as light sources, photodetectors), 2) Transmitter that controls the timing and intensity of the light sources, 3) Receiver, that collects the absorbed and reflected light from the tissues and sends them to the 4) control unit that is responsible for synchronized operation of the whole system (Figure 3.5).

The choice of the light sources, detectors, transmitter, and receiver determines the amount of the information deducible from the FOI system with several advantages and disadvantages.

As for comparison, each of the methods, CW, FD and TR, has its own advan-

tages and disadvantages outlined in Table 3.1. The choice of measurement method is determined by the type of the information that researchers seek.

Table 3.1
Comparison of the optical imaging systems [9].

METHOD	ADVANTAGES	DISADVANTAGES	INFORMATION COLLECTED
CONTINUOUS WAVE	Sampling Rate, Instrument size, Cost	Penetration Depth, Difficult to separate, absorption and scattering	Finger pulse oximeter, Neuroimaging studies
FREQUENCY DOMAIN	Sampling Rate, Relatively accurate separation of absorption and scattering	Penetration Depth	Cerebral and muscle oximetry, breast imaging, tissue characterization
TIME RESOLVED	Spatial resolution, Penetration Depth, Most accurate separation of absorption and scattering	Sampling rate, Instrument size, Stabilization, Cost	Imaging cerebral oxygenation and hemorrhage in neonates, breast imaging

There is a wide variety of instruments currently in use for both commercial and research applications. 1) Researchers at Hitachi (Tokyo, Japan) have built a continuous intensity system for the topographic mapping of cortical activity. The measurements were performed with a continuous wave optical imager system, which was placed on the head to obtain a topographic map. 2) An advanced 64-channel TCSPC (time-correlated single photon counting) system has been constructed as part of a Japanese MITI funded project. It is a time-resolved instrument that employs specially developed low power picosecond diode lasers (average power 0.25 mW) and fast PMT detectors. 3) Dr. D. Benaron's research group at Stanford University developed an optical imaging system that uses pulsed laser diode sources and either a commercially available Optical Time Domain Reflectometer (OTDR) or avalanche photodiode detectors (APD). 4) The group of Dr. B. Chance at the University of Pennsylvania,(a) have constructed

a continuous wave light optical imager that consists of ten detectors and four light sources arranged in an array. This device is placed on the forehead to measure the optical density changes during the brain activition. (b) Another system developed in Prof. Chance's group is an 8 channel time resolved TCSPC instrument is also developed. The system employs pulsed laser diodes at 780 and 830 nm to perform spatially resolved NIR spectroscopy for monitoring motor cortex activity, as well as performing tomographic breast phantom studies. 5) At Dartmouth College Dr. H. Jiang has developed both continuous intensity and frequency-domain optical imager. 6) At University College London, the research group, under the direction of Professor David Delpy, is involved with the development of new optical monitoring instruments based on Time-resolved optical imaging system for medical applications. 7) At Harvard Medical School, Dr. D. Boas's group has constructed a continuous wave optical imager. 8) Dr. Anreas Hielscher's biomedical optics group at Columbia University is developing numerical and experimental techniques for in vivo tissue diagnostics.

Meanwhile here at Boğaziçi University, Dr. Ata Akın, before initiating the project on this thesis, has been studying on improving the functional optical imager developed by Dr. Chance' group in Philadelphia. The modified CW fast optical imager system is described in chapter 4.

3.4 Need for Modified and Improved Optical Imager

The advantages that diffuse optical techniques can provide brain researchers are significant. These include portability, ease of application, reduced discomfort to subject, reduced emotional artifacts due to improved freedom of mobility and low cost. Like all techniques, these advantages come with some limitations, and so we consider here the issues that need to be improved and considered when designing a continuous wave optical imager.

Only two groups that are currently working on continuous wave optical imaging

systems have explained their design specifications in detail. Table 3.2 compares these systems. According to these specifications, several improvements and modifications are required for improved quantification of brain activation in neuroimaging studies. For instance, adjustable sampling rate with no added costs to system design leads to increase temporal resolution of the system. Reduced number of control channels also leads to an improvement in sampling rate and decreases the cost of the system and complexity.

Table 3.2
Comparison of the CW optical imaging systems.

	Number of Sources/Detectors	Sampling Rate	Cost	Dynamic Range
CW DOT(Diffuse Optical Tomography) (Boas's group)	18/16	40 kHz	Moderate	80 dB
CW fNIR (Chance' s group and Drexel University)	4/12	60 kHz	Low	Not Tested

Table 3.3
Comparison of the probes of the current optical imaging systems.(N/A : not Appicable)

	Comfort	Ease of Application	Robustness	Flexibility
CW fNIR(Chance' s group)	Low	Moderate	High	Low
CW fNIR(Drexel University)	Not Tested	NotTested	Moderate	High
CW FOI(at Boğaziçi University)	High	High	Not Tested	High
Other Optical Imagers	N/A	N/A	N/A	N/A

One other limitation of the CW optical imaging system is the current probe design. Source-detector separation changes with respect to variations in the skull anatomy. This yields a substantial error on detected signal. In Table 3.3, existing probes used in current functional optical imaging systems are compared. Therefore, probe design must be done by considering the probe flexibility with source detector distance fixation. By fixation of the source and detector, motion artifacts that cause large spikes on optical measurements can also be eliminated.

Finally, electronic hardware must be designed carefully. Any given detector is sensitive to all wavelengths of light, and there usually are many source colors and/or source locations to be monitored by any given detector. The electronics must therefore be engineered to allow separation of the various colors and locations. This is achieved by multiplexing the sources and detectors. During a quadrant based operation, reflected light can be monitored without generating cross-talk between sources.

4. SYSTEM DESIGN AND PERFORMANCE CHARACTERIZATION OF FAST OPTICAL IMAGER

This M.Sc. thesis is concerned with the development of a Continuous Wave Fast Optical Imager for functional brain imaging studies. While the first section of this chapter discusses the various considerations that led to its particular design, a detailed description of the overall system and its individual components are given in section 4.2. The most significant aspects relating to the system's performance are analyzed in section 4.3.

4.1 General System Considerations

It is the aim of this research to develop and construct an optical imager device in Turkey to enable neuroimaging studies with alternative methods[1] . The following points summarize the most important technical specifications of the CW imaging instrument that guided the development process.

Probe

- LEDs must work in near infrared spectrum. Each LED must have multiple wavelengths that emits at 730 nm for Hb and 850nm for HBO_2. Detectors should be sensitive in the NIR spectrum and must have high sensitivity for low level signals in order to estimate minute changes in cromophore concentrations.
- Probe where LED and detectors are placed on must fit around forehead of the subject. Flexibility of the probe and distance fixation for source detector separation must be achieved. Temperature increase and sweat secretion between skin and probe must be minimized.

System Control

[1] To the best of our knowledge, we are the first group to develop such a system in Turkey

- CW FOI can be fully controlled by 8 channels. Four of them are control channels and rest of them are for analog data collection channels. By using four control channels, we can control acquisition rate manually.

System Characteristics

- There should be negligible cross talk between channels. Only one LED must be on at each data collection interval. Quadrant based operation can accomplish this task.

- The system must be portable to allow preliminary clinical trials to be performed in hospitals.

- Low power consumption. This should allow for battery operation and a wearable design.

- System must be low cost. Competition in neuroimaging techniques demands for a low cost instrument as an alternative to fMRI and PET.

- Adjustable sampling rate. As for now, sampling rate for CW FOI systems has not been optimized. By giving the possibility of adjusting the sampling rate, different physiologic events will be monitored.

4.2 Instrument Description

The CW system that is developed in this thesis is based on the system in University of Pennsylvania. In figure 3.5 and 4.1, a block diagram of the CW FOI system is illustrated. CW FOI device has four important parts. These are 1) Probe, 2) Control Unit (includes DAQ card, PC), 3) Transmitter Circuit and 4) Receiver.

Figure 4.1 A picture of CW FOI .

4.2.1 Probe

The probe houses light sources, photodetectors and special backing and band material.

Light sources used in this thesis are multi-wavelength light-emitting diodes (L4*730/4*805/4*850-40Q96-I, EPITEX, Japan). They emit in NIR spectrum at 730nm, 805nm and 850nm (Figure 4.4(a)).

Detector options ranged from multi-anode PMTs(Photomultiplier Tube) to discrete commercial-grade photodiodes with external preamplifiers. A monolithic photodiode/preamplifier IC housed in a clear 8-pin DIP package (OPT101 from Burr-Brown) is used (Figure 4.4(b)). This offered both the convenience and low-cost of a solid-state detector, combined with the electrical and optical isolation of an integrated preamplifier. The simplicity and the less stringent electrical shielding requirements for the monolithic preamp influence the decision.

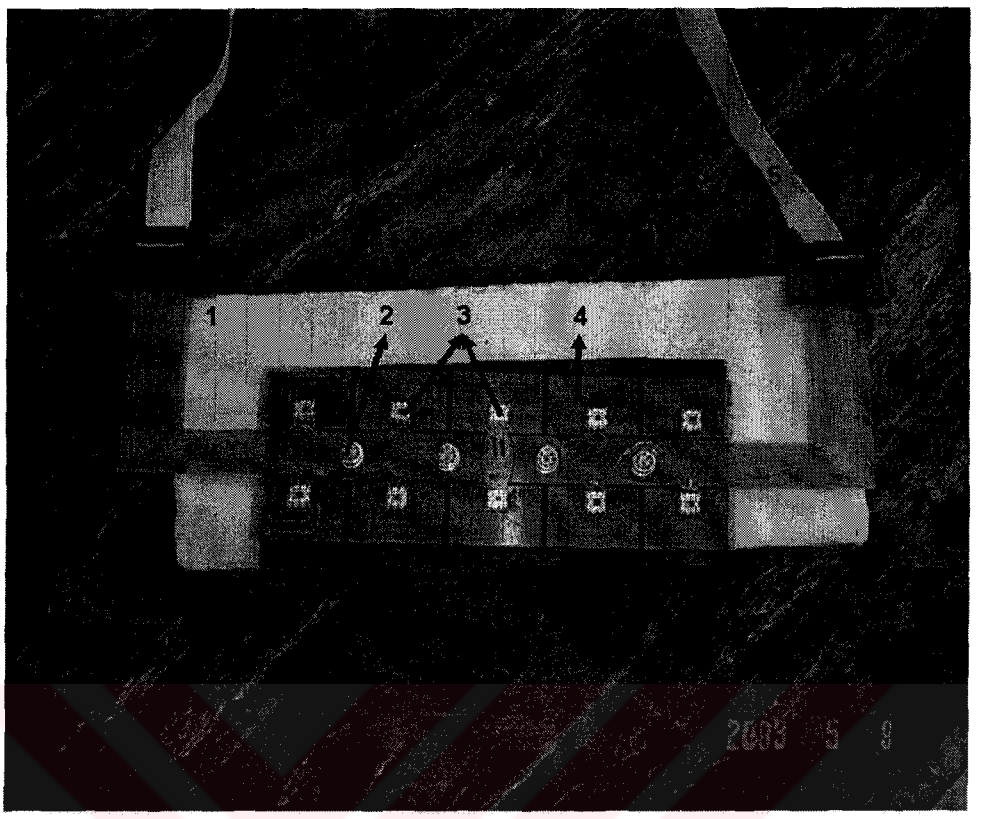

Figure 4.2 Designed probe. 1) Phantom, 2) LED, 3) Photodetectors, 4) PCB, 5) Connectors.

The photodiodes in the probe detect changes in absorption at each wavelength during brain activation. It consists of four LEDs and ten detectors that require external control for their operation.Previous versions of CW FOI probe has been reported to have several problems. Flexibility and non-uniform pressure on subject forehead are main problems. In this thesis a new probe is designed by considering these problems.

According to these, designed probe is manufactured from flexible PCB that provides flexibility, robustness and covers subject head easily without using any covering band (Figure 4.2). In order to distribute the pressure on the subject skull uniformly, Sphygmomanometer Cuff is used(Figure 4.3(a)). Sphygmomanometer Cuff covers the probe and probe is placed on subject forehead. Then Sphygmomanometer Cuff is inflated by a hand bulb. As a result, uniform pressure on subject forehead is assumed to be maintained [2] (Figure 4.3(b)). Source detector distance in designed probe is 2.5

[2]This statement has not been tested due to the late arrival of the probe form the manufacturer.

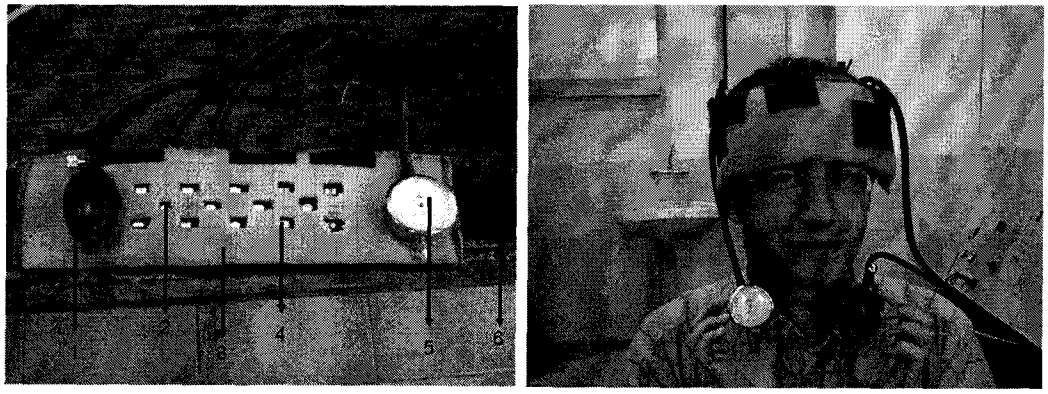

(a) (b)

Figure 4.3 (a)Designed probe with Sphygmomanometer Cuff: 1) Hand bulb, 2) LED, 3) Backing material, 4) Photodetector, 5) Sphygmanometer, 6) Band material. (b)An illustration for probe using .

cm like the previous probe.

4.2.2 Control Unit

Control unit includes both computer and DAQ card. Any computer which is compatible with Windows 2000 upper versions can be used. As for DAQ card, National Instrument NI PCI-MIO-16E-4 card is used. This card provides up to 250 kS/s multichannel sampling rate. We use only four of the digital outputs and analog input channels of the DAQ card to control the system. DAQ card can be controlled either by LabVIEW or Visual C++. We decided to use Visual C++ to eliminate any other software interference as it is the case with LabVIEW. In Figure 4.5, BRAINFO program that controls and monitors detected signals is shown.

The programming routine that software follows is based on turning on and off LEDs and sampling the detected signals to the computer. There are a total of 10 photodiodes and four LEDs on the probe. Due to the specific quadrant based multiplexing scheme, there are a total of 16 photodetector outputs and each window on software interface corresponds to these outputs, one for each of four LEDs, in

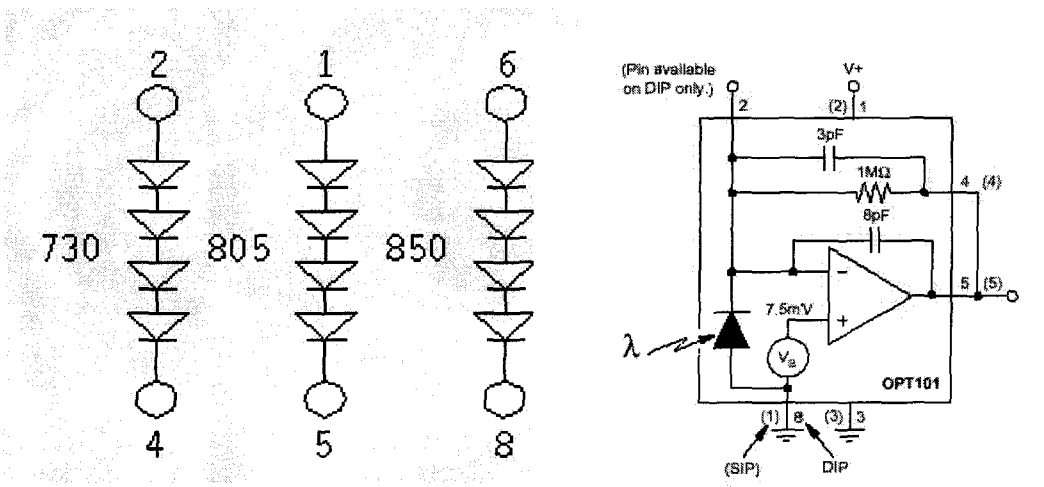

(a) (b)

Figure 4.4 (a)LED used in CW FOI.(b)Internal circuit diagram of OPT101.

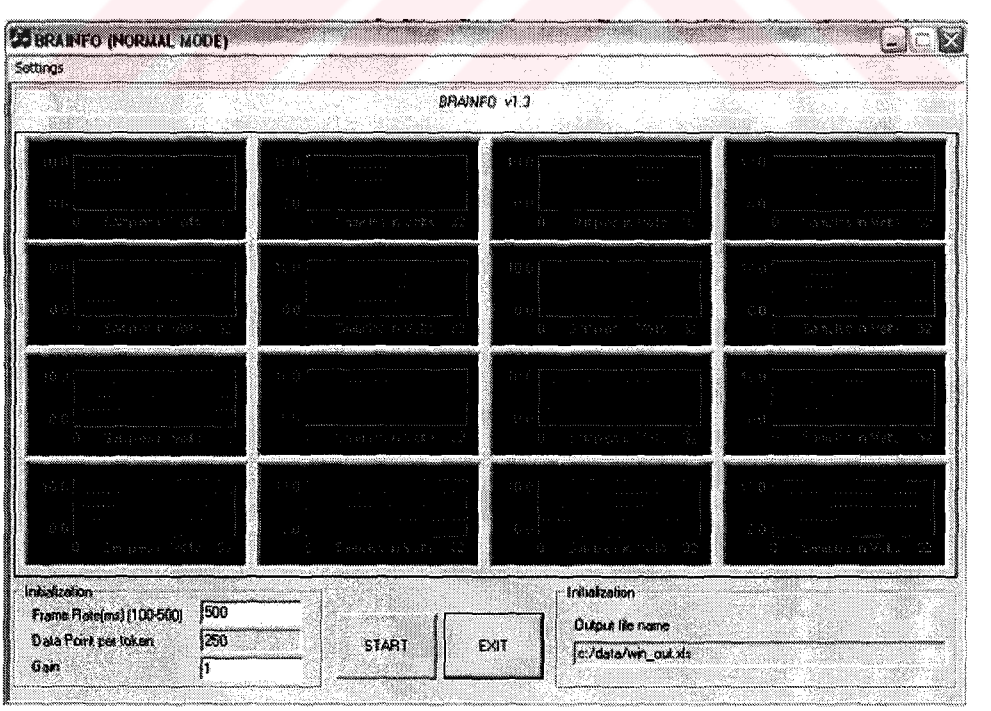

Figure 4.5 Software interface .

groups of 4 photodiodes. This means that all, except the outer left and outer right photodiodes are used twice, in pairs of 4. The order of sampling for each LED, then for each photodiode number (PD#) is:

- LED 1: PD# 1, 2, 3, 4;
- LED 2: PD# 3, 4, 5, 6
- LED 3: PD# 5, 6, 7, 8
- LED 4: PD# 7, 8, 9, 10

There are 3 wavelengths in each LED, the real sequence is: Q1

- Turn on LED 1, 730nm: sample PD# 1, 2, 3, 4;
- Turn on LED 1, 805nm: sample PD# 1, 2, 3, 4;
- Turn on LED 1, 850nm: sample PD# 1, 2, 3, 4;

Q2

- Turn on LED 2, 730nm: sample PD# 3, 4, 5, 6;
- Turn on LED 2, 805nm: sample PD# 3, 4, 5, 6;
- Turn on LED 2, 850nm: sample PD# 3, 4, 5, 6;

Q3

- Turn on LED 3, 730nm: sample PD# 5, 6, 7, 8;
- Turn on LED 3, 805nm: sample PD# 5, 6, 7, 8;

- Turn on LED 3, 850nm: sample PD# 5, 6, 7, 8;

Q4

- Turn on LED 4, 730nm: sample PD# 7, 8, 9, 10;
- Turn on LED 4, 805nm: sample PD# 7, 8, 9, 10;
- Turn on LED 4, 850nm: sample PD# 7, 8, 9, 10;

BRAININFO program completes all processes in 400ms or less if desired.

4.2.3 Transmitter Circuit

Transmitter circuit has three functions in CW FOI system. These are quadrant selection, wavelength selection and LED current control.

Quadrant and wavelength selection are multiplexing processes controlled by PC and DAQ card. Four digital output channels are used to control digital timing circuit that controls operation timing of LEDs (Figure 4.6). Selection is done by two 2 x 4 multiplexers (MAX309). Truth table of the selection process is outlined below, Table 4.1 and 4.2. Multiplexer output is applied to logic AND gate (4081). Output of the AND gates trigger switches (MAX333) in order to turn LED driver circuits on(Figure 4.7). LED driver circuit is a constant current circuit based on an operational amplifier(Figure 4.8).

4.2.4 Reciever

Receiver circuit chooses the correct quadrant and collects data from the photodiodes and sends them to DAQ card and PC. Same, control signals mentioned in

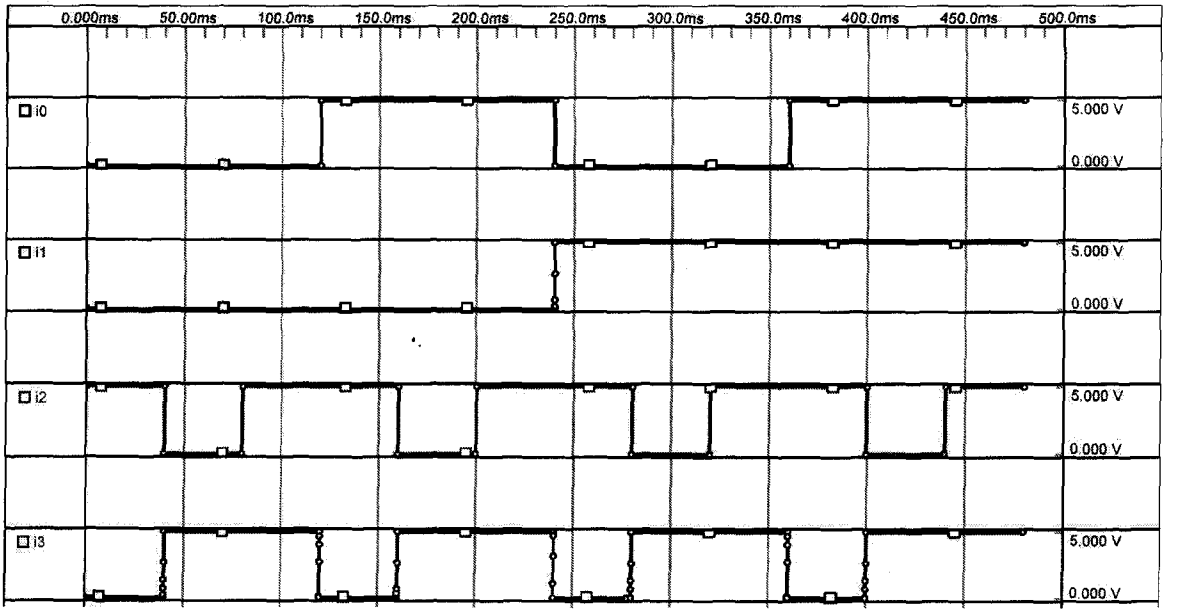

Figure 4.6 Control signals.

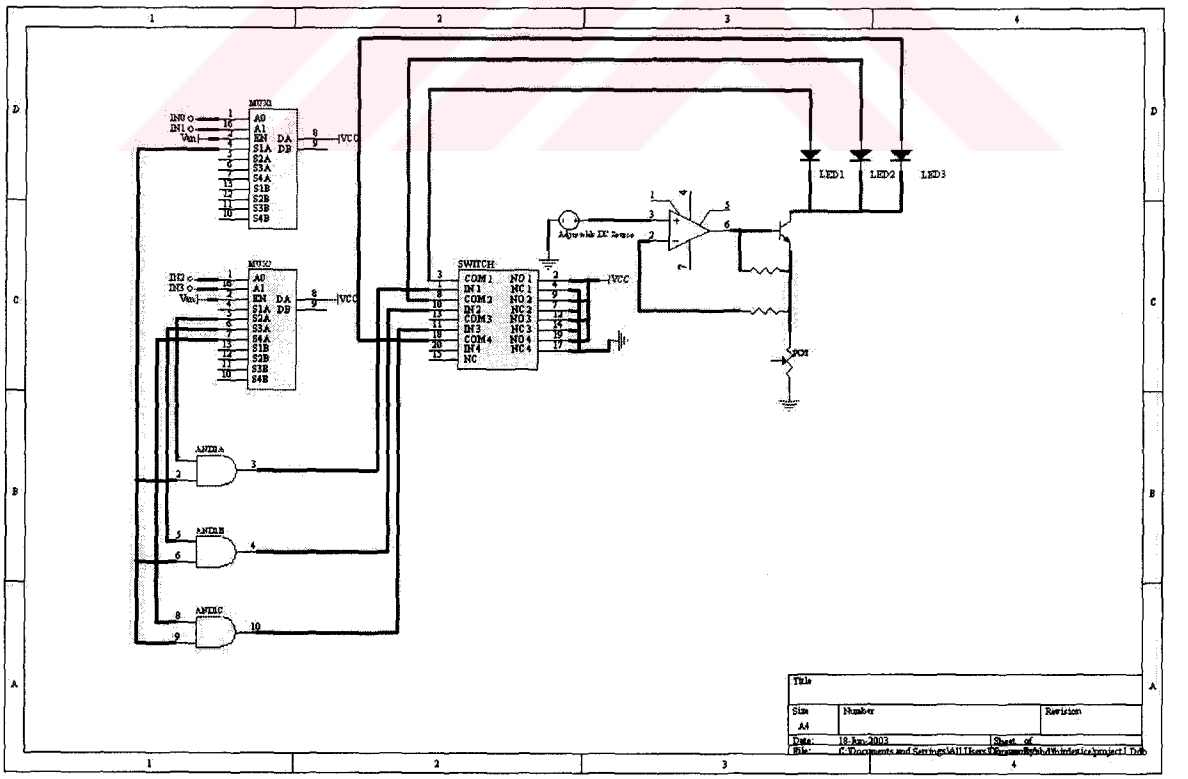

Figure 4.7 Schematic of transmitter circuit for quadrant one.

Table 4.1
Truth table for quadrant selection .

I0	I1	A0	A1	A2	A3	QUAD
0	0	1	0	0	0	Q1
1	0	0	1	0	0	Q2
0	1	0	0	1	0	Q3
1	1	0	0	0	1	Q4

Table 4.2
Truth table for wavelength selection.

I2	I3	A0	A1	A2	A3	WAVELENGTH
0	0	1	0	0	0	RESET
1	0	0	1	0	0	λ 1
0	1	0	0	1	0	λ 2
1	1	0	0	0	1	λ 3

transmitter circuit are used. Continuously, 10 detectors send signals to receiver circuit. Receiver circuit selects quadrant and wavelength and then transmits to DAQ card. Bidirectional multiplexers (MAX309) are used for quadrant and wavelength selection (Figure 4.9).

4.3 System Performance

4.3.1 Led Power Measurement

Incident power of the CW FOI device is important in order to compensate loss of emitted signal during the propagation in tissue. Because detected signals are typically on the order of 10 pW for a source-detector separation of 4 cm, or a loss of 7-9 orders of magnitude in light power as it is reported before [9] .Therefore, to increase signal to noise ratio (SNR) of this device we have to increase incident LED power. The LED output power should be proportional to injected current. In order to characterize

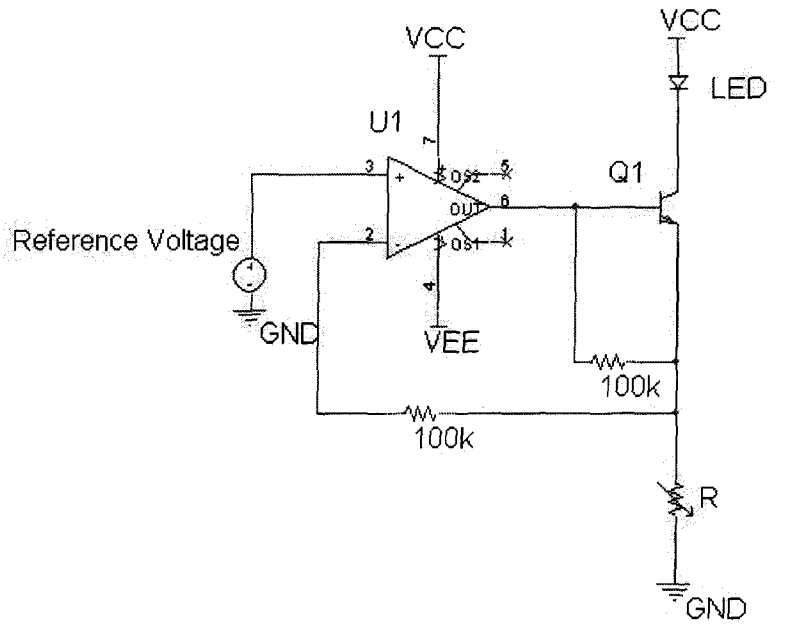

Figure 4.8 Schematic of LED driver circuit.

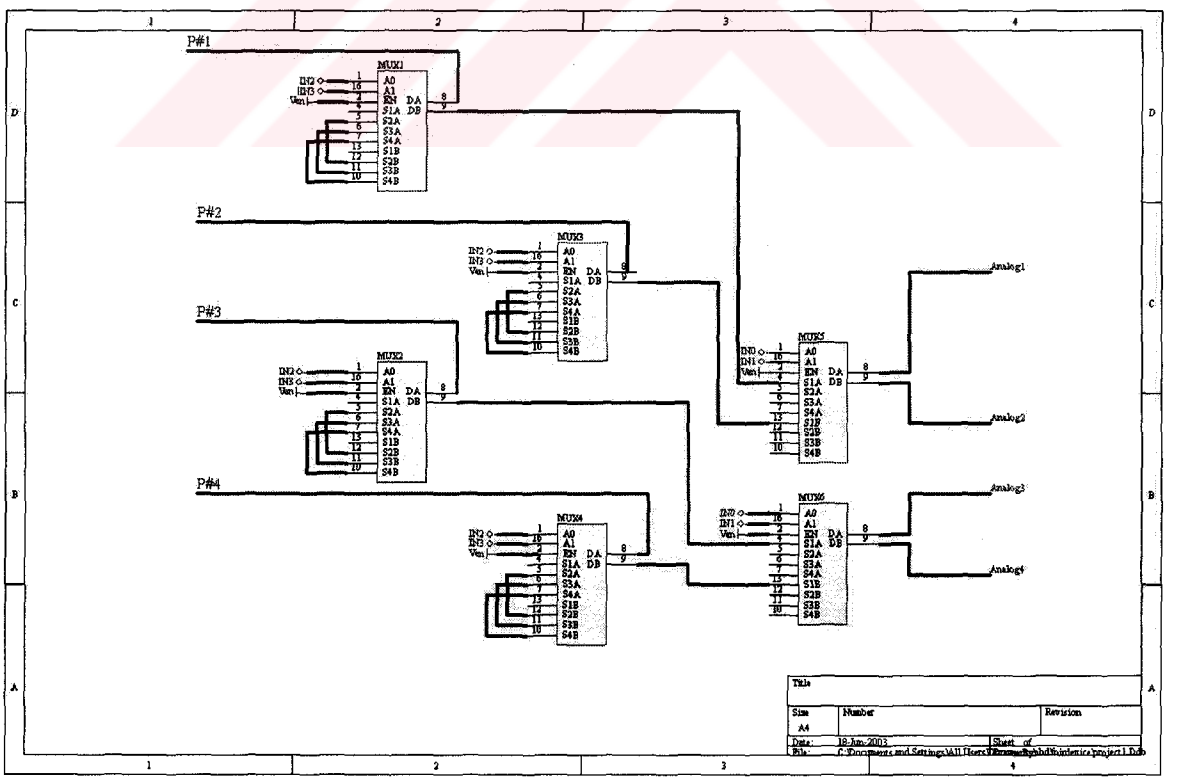

Figure 4.9 Schematic of receiver circuit for quadrant one.

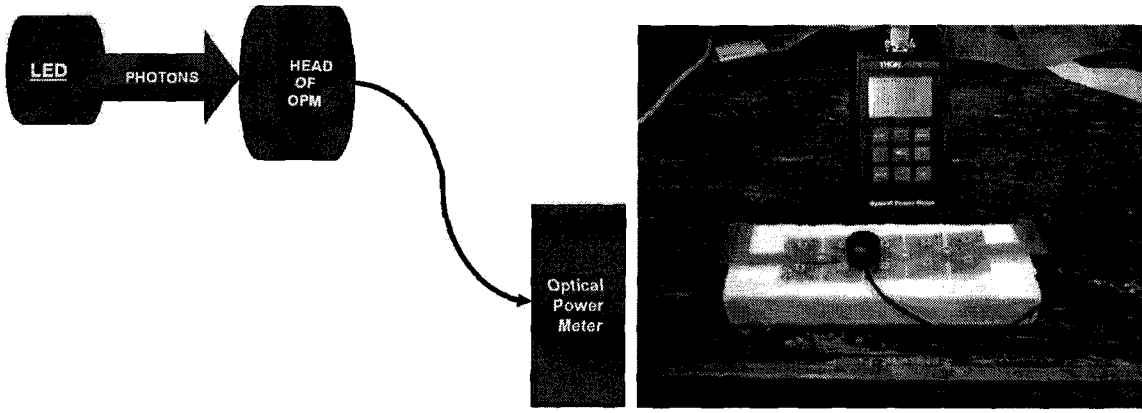

(a) (b)

Figure 4.10 (a)Block diagram for LED power measurement(b) Experimental setup for LED power measurement .

current and LED power relationship in this system following experimental procedure is applied. Experimental setup illustrated in figure 4.10(a) is built up(Figure 4.10(b)).

Experimental Procedure:

- Connect the LED to the current source.
- Adjust the current limit to 50mA
- Place the power meter as close as possible the LED and cover with a black cloth.
- Measure the current and output power of the LED in 2 mA steps from 0-20mA.
- Plot power output vs. current.

Results are presented for one LED in Figure 4.11.

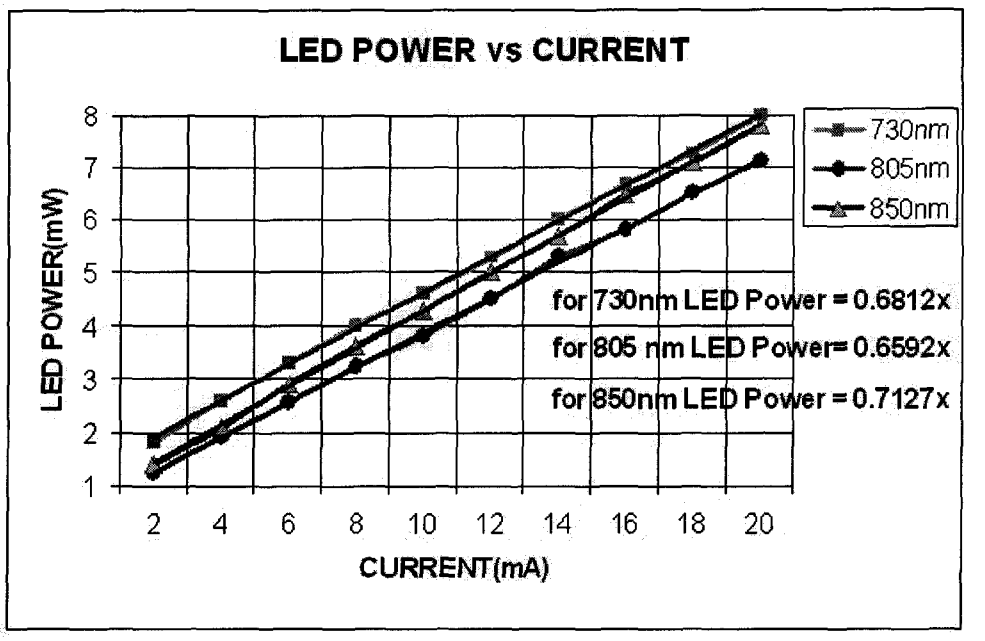

Figure 4.11 LED power vs LED current

4.3.2 Stability

We measured stability for LED output power and power supply. During the LED power experiment,a decrease of LED forward current was observed. When the LED is continuously on, temperature increases and this results as a drop of both forward current and output power. Figure 4.12(a) taken from datasheet of LED shows the LED Current changes with respect to temperature. Figure 4.12(b) is the experimental result of forward current change in 2 minutes.

Power supply stability is also important because if dc output of the power supply has fluctuations, these fluctuations can couple to all of the component outputs in the circuit. In order to overcome this problem 12 V, 1.3 AH rechargeable battery is used.

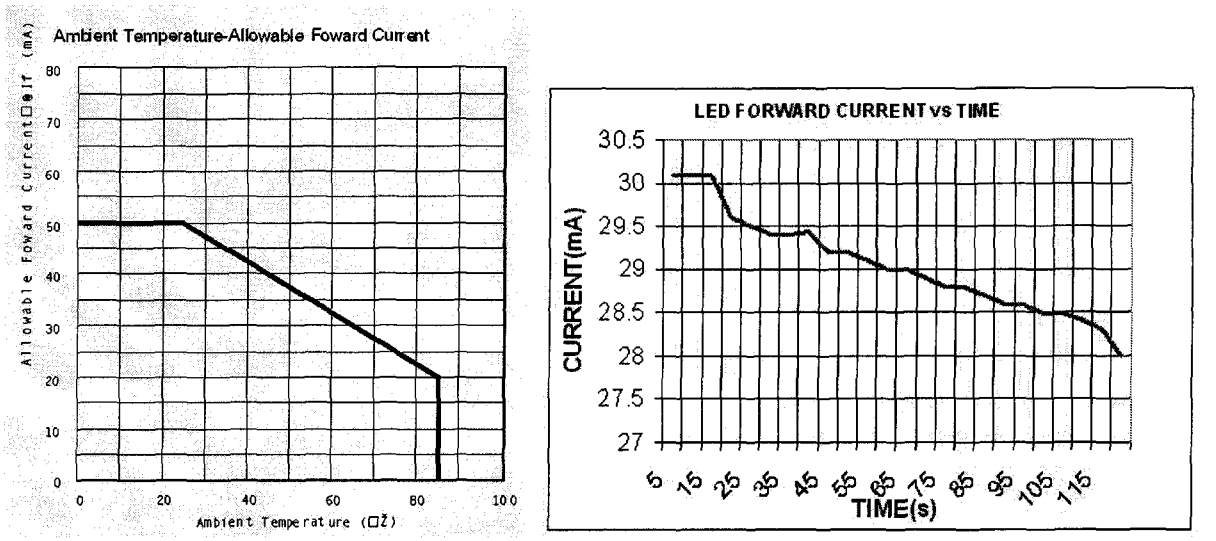

(a) (b)

Figure 4.12 (a)LED forward current vs. Temperature (Epitex datasheet). (b)Measured LED forward current changes as the temperature increases.

4.3.3 Background Noise

Most of the noise interference occurs at probe or detectors. Denoising the noisy signal is difficult at this level of the system due to the very low level signal of detectors. Therefore, noise characterization of photodetectors is an important study to understand observed signal.

Two main factors must be considered in the noise model of a photdetector. One of them is photon noise and the other is environmental noise. In this thesis we only investigated environmental noise. Our assumption for environmental noise is white noise (N, σ).Hence, noise model formula is given below.

$$n_{det} = n_{env}^{on} + n_{env}^{off} \tag{4.1}$$

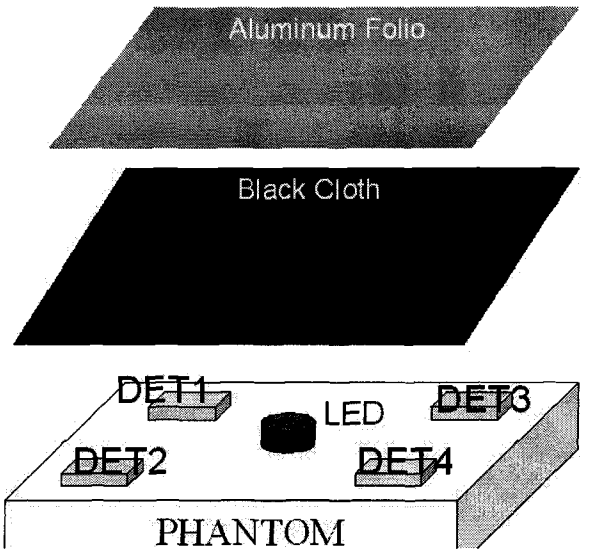

Figure 4.13 Block diagram for experimental setup

Photodetector noise (n_{det}) is equal to sum of background noise when the LEDs are off (n_{env}^{off}) and added noise when the LEDs are on(n_{env}^{on}).

We used a phantom with optical properties similar to those of the brain. We covered the probe with a black cloth to eliminate background light, and covered whole experimental setup with aluminum folio in order isolate power line interference. Figure 4.13 illustrates the experimental setup.

First we measured detector outputs when the LEDs were off. While the detectors were covered with black cloth, we measured voltage at the output of the detectors. We called this as baseline noise level. Table 4.3 shows the results of the measurement done for base line noise.

Table 4.3
Mean and standard deviation of photodetectors when the LEDs were off

	DET1	DET2	DET3	DET4
μ	14mV	14.3mV	14.4mV	14.4mV
σ	5mV	4.9mV	4.8mV	4.8mV

When LEDs are on, we applied experiment procedure outlined below:

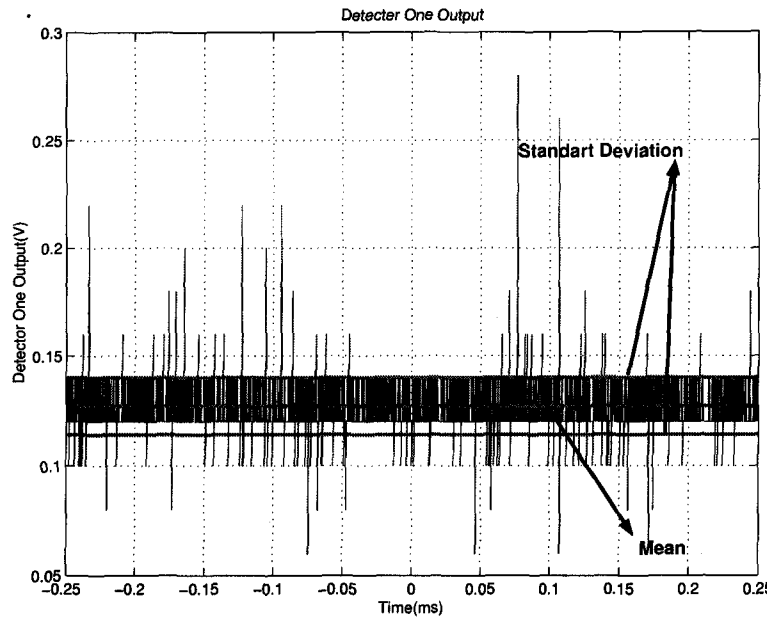

Figure 4.14 Standard deviation of noise intensity for four photodetectors.

- Increase the LED driver circuit current from 2 mA to 24 mA.
- For each current we define noise intensity (N_d) as standard deviation of detector output(Figure 4.14).
- This process was applied 10 times and standard deviation of noise intensity is calculated(Figure 4.15).

As can be seen from the figures, noise intensity is almost constant for every LED current. Increasing the LED current does not change the detector Noise intensity. When we combine on state results with base line noise level, base line noise increases maximum of 4 mV. This result is an evidence for an additive noise at the detector output while the LEDs are on.

In order clarify our white noise assumption, we look at the PDF (probability density function) of the detected signal and compare with the white noise PDF (Figure 4.16). The figure indicates that noise component of the detected signal is not white noise but this does not affect the preceding results, because Noise intensity is found to be constant at every LED current.

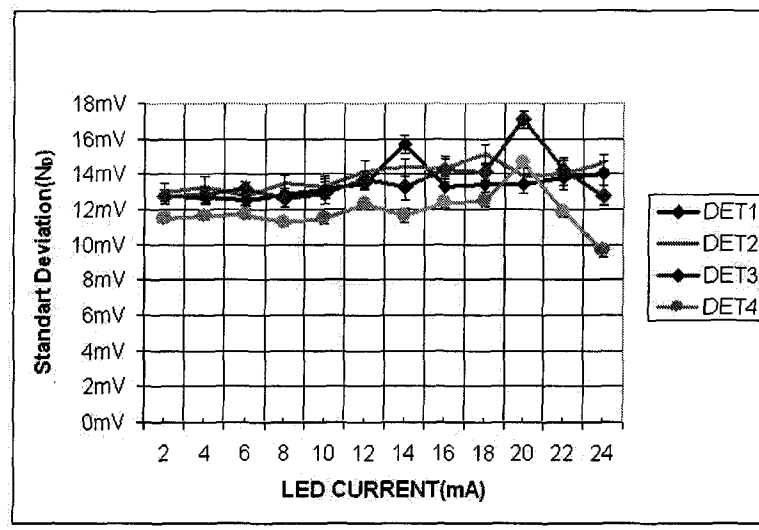

Figure 4.15 Detector one output when the LEDs were on.

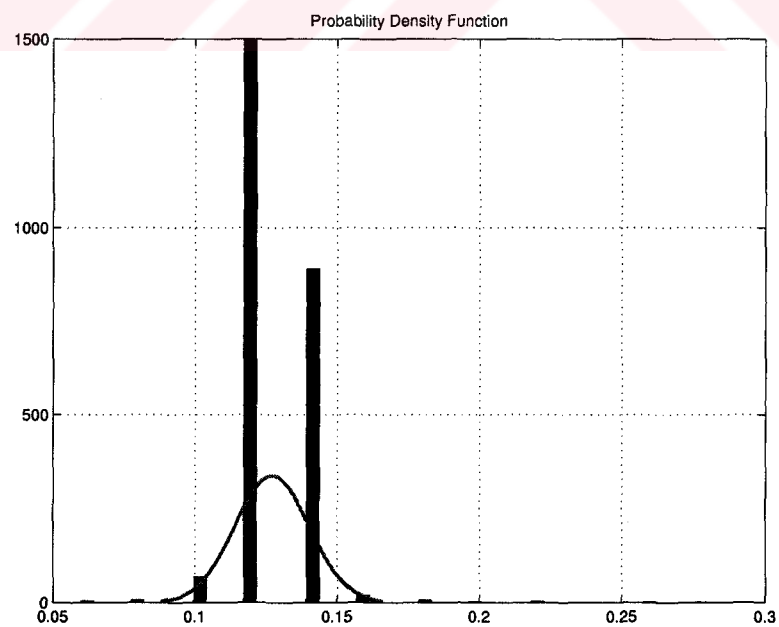

Figure 4.16 PDF of photodetector output

5. Conclusions

The current state of this research project and likely future work are reviewed in this final chapter.

A modified duplicate of CW FOI of University of Pennsylvania has been constructed and evaluated. Portability, low cost and adjustable sampling rate is achieved. Its performance is evaluated from the preliminary data obtained from phantom studies.

It has been reported that typical signal levels detected from the brain studies is around 1.5 V. Electronic noise of the CW FOI is measured to be 15mV. This noise level is found to be independent from the operation conditions of the system such as LED current driver and sampling rate. A quick SNR calculation from these results provide us a SNR value of 40 dB.

5.1 Recommendations for Future Work

Future work will focus on further improving the system's performance and prospects for the commercial and clinical utilization of the CW FOI technology.

Characterization of the designed probe is very important. Pressure vs. SNR measurement and comfort level tests must be the aim of future studies.

LEDs temperature is observed to be a significant factor that determines the light intensity on the forehead of the subject. Therefore, operation temperature measurement of the LEDs must also be accounted for in future studies.

Using advanced DAQ card provides higher temporal resolution.

Improving the PCB design will reduce the dimension of the CW FOI system.

We are planning on further improving the SNR by performing an averaging operation.

In the near future, we believe that the parallel advances seen in EEG, fNIR, the computational processing power of computers, and in the identification/understanding of cognitive processing centers of the human brain is bound to create sophisticated tools for cognitive neuroscience research [14].

REFERENCES

1. Raichle, M. E., "Behind The Scenes of Functional Brain Imaging: A Historical and Physiological Perspective," *Proc. Natl. Acad. Sci.*, Vol. 95, pp. 765–772, 1998.

2. Frackowiak, R., P. J. Magistretti, R. Shulman, J. Altman, and M. Adams, "Neuroenergetics: Relevance for Functional Brain Imaging," Workshop XI, Human Frontier Science Program, Strasbourg, 2001.

3. Malmivuo, J., "Theoretical Limits of The EEG Method Are Not Yet Reached," *International journal of Bioelectromagnetism*, Vol. 1, no. 1, pp. 2–3, 1999.

4. Paetau, R., "Magnetoencephalography in Pediatric Neuroimaging," *Developmental Sciences*, Vol. 5, no. 3, pp. 361–370, 2002.

5. Magisretti, P. J., *Fundamental Neuroscience*, Elsevier Science, California, USA, 2nd ed., 2002.

6. Magistretti, P. J., and L. Pellerin, "Cellular Mechanisms of Brain Enegry Metabolism and Their Relevance to Functional Brain Imaging," *Phil. Trans. R. Soc. Lond. B*, Vol. 354, pp. 1155–1163, 1999.

7. Chance, B., M. Cope, E. Gratton, N. Ramanujam, and B. Tromberg, "Phase Measurements of Light Absorption and Scatter in Human Tissue," *Rev. Sci. Instru.*, Vol. 69, no. 10, pp. 3457–3481, 1998.

8. http://www.hitachimed.com/products/. "Optical Topography System"

9. Strangman, G., D. Boas, and J. Sutton, "Non-invasive Neuroimaging Using Near-Infrared Light," *Society of Biological Psychiatry*, Vol. 17, pp. 679–693, 2002.

10. Meek, J., "Basic Prinicples of Optical Imaging and Application to The Infant development," *Developmental Science*, Vol. 3, no. 3, pp. 371–380, 2002.

11. Tuchin, V., *Tissue Optics*, Spie Press, Washington,USA, 2000.

12. Schmidt, F. E. W., "Development of a Time-Resolved Optical Tomography System for Neonatal Brain Imaging," Ph.D. thesis, University College London, London, England, 1999.

13. Hirtz, D. G., A. Gandjbakhche, L. Wright, and B. Chance, "Workshop on Near Infrared Spectroscopy in Infants and Children," Workshop, National Institute of Neurological Disorders and Stroke and National Institute of Child Health and Human Development, Bethesda, Maryland, 2001.

14. Kruse, A., and D. Schmorrow, "What can Modern Neuroscience Technologies Offer The Forward-Looking Applied Military Psychologist?," *Symposium IAMPS2002*, 2002.

15. Strangman, G., J. P. Culver, J. H. Thompson, and D. A. Boas, "A Quantitative Comparison of Simultaneous BOLD fMRI and NIRS Recordings During Functional Brain Activation," *NeuroImage*, Vol. 17, pp. 719–731, 2002.